Particle Image Velocimetry of a Y-bifurcator

W. Dobler[1] and G. Zenz[1]
[1]Institute of Hydraulic Engineering and Water Resources Management
Graz University of Technology
Graz, 8010
AUSTRIA
E-mail: w.dobler@tugraz.at

Abstract: *In this paper PIV-Measurements are presented for a Y-bifurcator of a power plant. The Plexiglas model test consists of a 42 degree bend, a straight pipe from the bend to the Y-branch and two branching pipes with a branching angle of 40 degrees. At several locations PIV-Measurements upstream and downstream of the Y-bifurcator are carried out by using natural seeding particles. The quality of the seeding particles will be presented by means of the velocity lag and the size of the particles. A confidence interval for a typical PIV-Measurement is calculated to demonstrate the reliability of the mean velocity. The result of the PIV-Measurement shows the velocity profile and the secondary flow within the Plexiglas installation. The secondary flow will also be quantified by the velocity correction factor α. Due to the reflection at the Plexiglas surface, the velocity profile will be closed with a linear function. The accuracy of this procedure will be checked with a CFD calculation.*

Keywords: *Hydraulic model test, Particle Image Velocimetry (PIV), secondary flow, velocity correction factor, numerical simulation*

1. INTRODUCTION

As is well-known a pipeline between a reservoir and a power plant is necessary to transport the water in the shortest way to the power plant, with low energy losses and with economical low prized pipe installation. The penstock consists therefore mostly of a single pipe which distributes the water - shortly before the power plant - to several turbines. The distribution is in many cases done by a Y-bifurcator which is investigated by numerous authors, like (King, 1963), (Lee *et a*l, 1993), (Ruus, 1970) and (Williamson & Rhone, 1973). In the Hermann Grengg Laboratory a 8.13 times smaller hydraulic model test of a Y-bifurcator is set up to investigate the hydraulic behavior of a dividing flow. As a further challenge, a bend is located 18 times the diameter upstream of the Y-bifurcator which causes a slight secondary flow in the pipe installation (see Figure 1). This makes it necessary to get more information of the velocity and pressure distribution along the pipe installation of the hydraulic model test. With the Bernoulli-Equation it is possible to calculate the head loss between two control sections up- and downstream of the bifurcator. With

$$z_1 + \beta_1 \frac{P_1}{g\,\varrho} + \alpha_1 \frac{V_1^2}{2\,g} = z_2 + \beta_2 \frac{P_2}{g\,\varrho} + \alpha_2 \frac{V_2^2}{2\,g} + h_l \qquad (1)$$

one can calculate the head loss h_l, whereas z is the geodetic height, β the pressure correction factor, P the static pressure, α the velocity correction factor, g the gravity and final V the mean velocity in the pipe. The index 1 and 2 denotes a control section before and after the Y-bifurcator where the mean velocity V and the pressure P can be measured with flow meters and pressure probes, respectively (see also the previous paper (Dobler *et a*l, 2010) for this hydraulic model test). The pressure correction factor β is zero because no strong curved streamline occur in the control sections (apart from the bend). The velocity correction factor α, which quantifies the axial secondary flow, will be closer investigated by means of PIV. The discharge rate for the bifurcation is either 160 l/s (each branch 80 l/s) or 80 l/s (the flow streams only through the left branch).

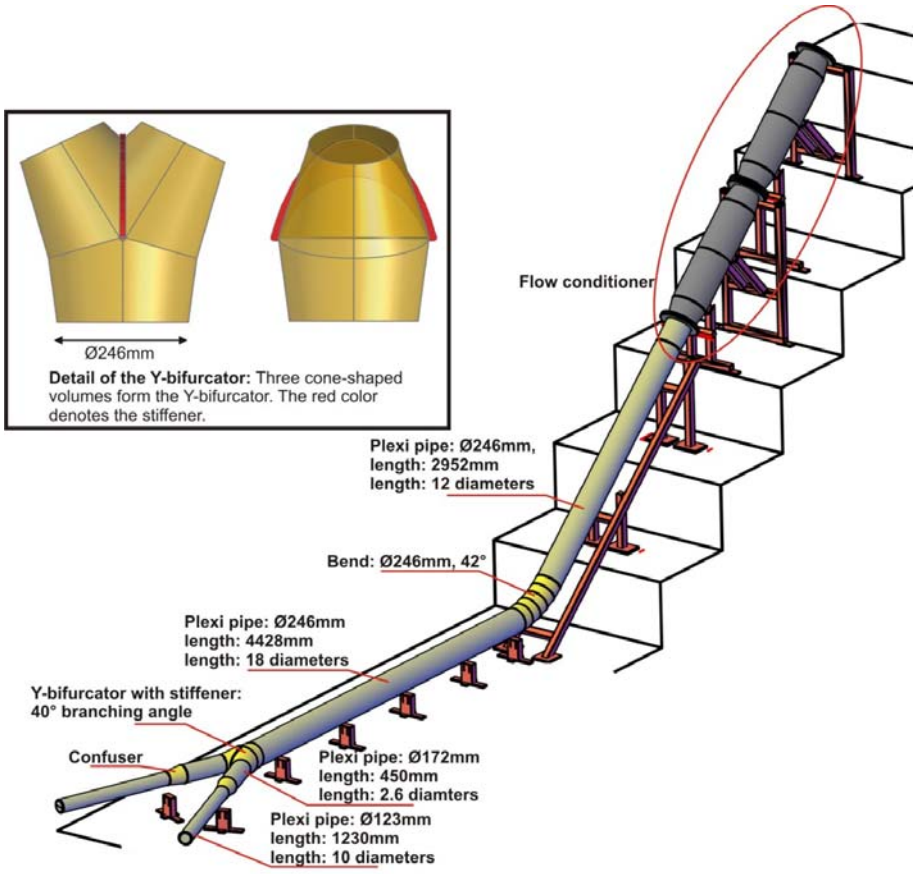

Figure 1 Set up of the hydraulic model test

2. SET UP FOR PIV-MEASUREMENTS

Particle Image Velocimetry (PIV) is an optical method to obtain instantaneous velocity vector fields of a 2D-Plane within a fluid. The positions for the measurements are shown in Figure 2. For each PIV-Box four planes are available to investigate the axial velocity.

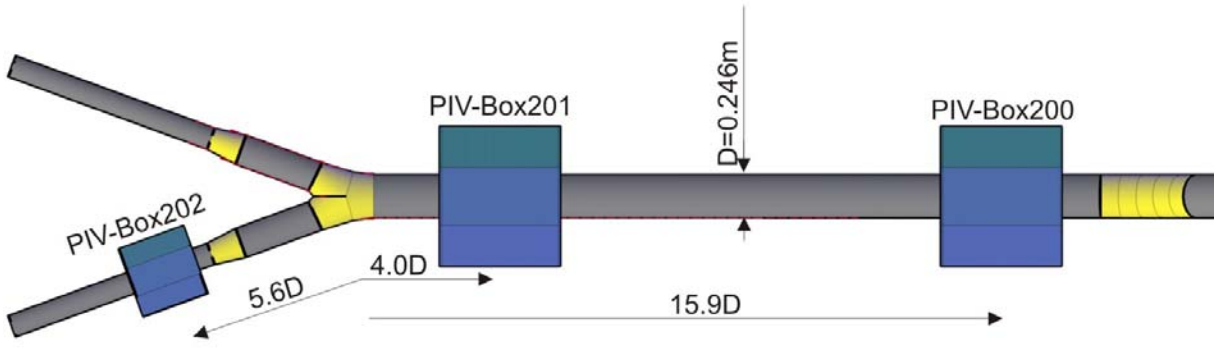

Figure 2 Position for PIV-Box to measure the axial velocities

The laser for the PIV-measurement is a Litron Laser – Model (LDY303-PIV) with a repetition rate of 0.2 – 10 kHz with 21.5 – 1.85 mJ. The wave length is 527 nm (green light). The camera is a Photron FASTCAM SA-1 with a frame rate of 5.4 kHz and resolution of 1024 times 1024 pixel. The working memory has a storage capacity of 16 GB. For a measurement the camera is normally oriented to the 2D-Laser light sheet (see Figure 3, left) and all the illuminated particles (seeding) are recorded. With the images from the camera a cross correlation is done to get the velocity vector field.

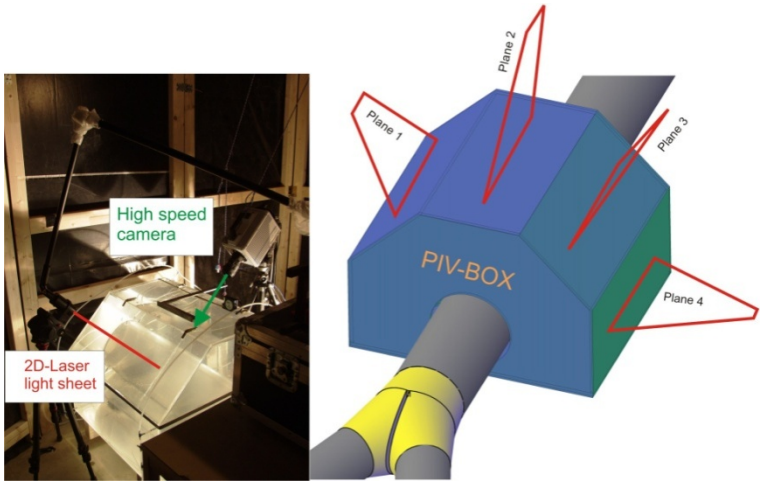

Figure 3: PIV-Box (filled up with water) to avoid the astigmatism effect of the curved pipe surface. Four planes are available to measure the axial velocity

2.1. Natural seeding

Du to the size of the hydraulic model test and the reservoir for the water supply it is not possible to add seeding with a certain property (density, diameter...) to the flow. Therefore, natural seeding are used to measure the velocity within the pipe. To estimate the quality of the natural seeding the average size and the density of the seeding is necessary.

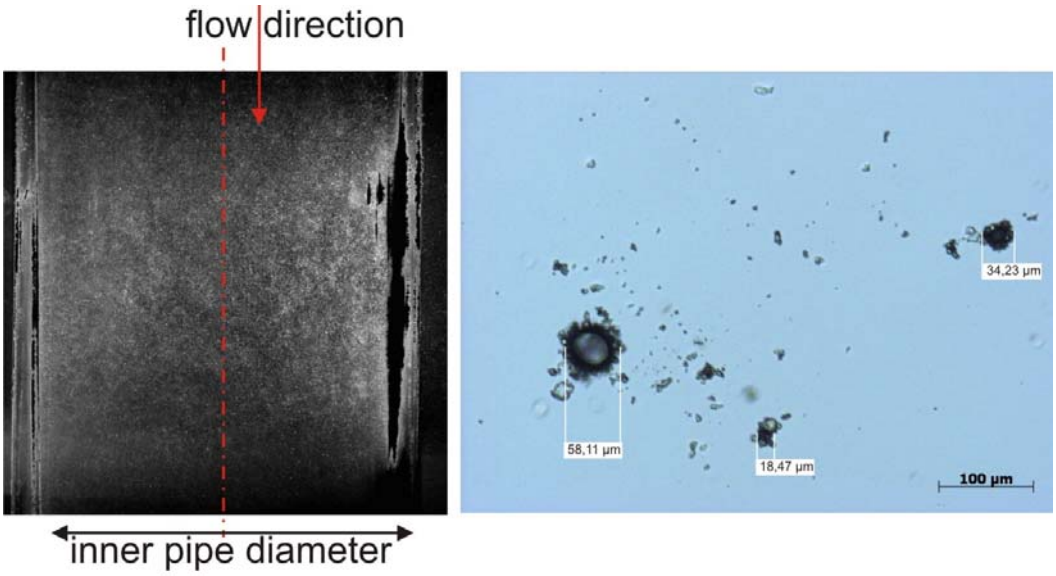

Figure 4 The picture on the left shows the raw data of an instantaneous PIV-measurement where the mean value of the gray levels is subtracted. The picture on the right shows the natural seeding with an optical microscope.

Figure 4 shows a representative example image of a PIV-measurement right after the bend (PIV-BOX 200, Plane 4), where the natural seeding can clearly be distinguished. The diameter of the natural seeding is determined by using a microscope (see Figure 4, right). Several probes had been taken from the water reservoir to check the particle diameter. In the majority of cases the particle size was between 20 and 50 micrometer.

2.2. Velocity Lag of the natural seeding

PIV measures the velocity of the natural seeding and not of the actual flow velocity, carrying the

natural seeding. Every particle, depending on the size and density of the particle, has a velocity lag. One of the methods to estimate the velocity lag in a laminar flow for a spherical particle within a constant acceleration can be made by using the law of Stokes where the forces for gravity, buoyancy, resistance and inertia are in equilibrium (see also (Raffel *et a*l, 2007)). With

$$u_p = u_{end}\left(1 - e^{-\frac{t}{\psi}}\right) \tag{2}$$

and

$$\psi = \frac{2\ \rho_p\ r^2}{9\ \rho_f\ \upsilon} \tag{3}$$

gives the particle velocity u_p depending on the time t. The other variables are u_{end} which is the end velocity, ψ the relaxation time, ρ_p the density of the seeding, ρ_f the density of the fluid, υ the kinematic viscosity, r the seeding diameter and finale g the gravity. The density for the particle was estimated by using a lower and upper limit of 800 and 1200 kg/m^3. This definition is based on the consideration that only floating particles (density close to water) can be drawn in by the pumps in the reservoir. The diameter of the seeding particle is 50 micrometer which represents the upper limit from the investigation with the optical microscope. The result for the end velocity u_p is shown Figure 5. The particle reaches the end velocity, for example 1 m/s, depending on the density, in approximately 7 10^{-4} seconds (for other end velocity u_p the same time is needed). This result can also be interpreted as having a low pass filter where every turbulent frequency which is higher than 1.4 kHz is blocked due to the inability of the particles (velocity lag) to follow the higher frequency of the flow.

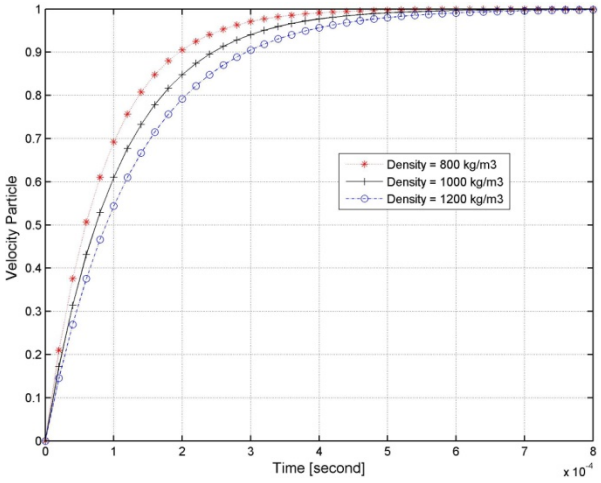

Figure 5 Time response of the natural seeding in accelerating flow

2.3. Confidence interval

With the software of Dantec Dynamics 2.20.18 the raw date with a recording time of at least 1 second and a frame rate between 1000 and 3000 will be evaluated to eliminate any outlier (these are peak, range and moving average validation, the recording time in the pretests was longer to check convergence). After that, the statistical accuracy of the steady state flow of the measurement is checked by a confidence interval with a t-distribution. This implies that the data are nearly normal distributed which will be demonstrated with the red marked example point in Figure 6.
With a confidence level of (1-α)=95% the reliability of the mean value, based on a t-distribution, is

$$\left[u - t_{1-\alpha/2}(n-1)\frac{S}{\sqrt{n}},\ u + t_{1-\alpha/2}(n-1)\frac{S}{\sqrt{n}}\right] \tag{4}$$

whereas u is the mean velocity, n the sample size and S the standard deviation.

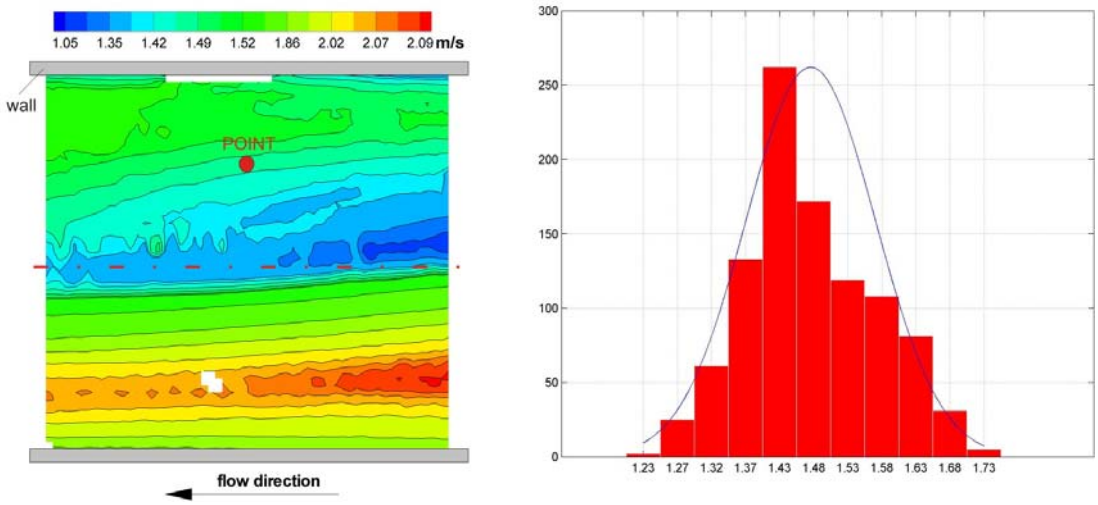

Figure 6 The right figure shows the histogram of the nearly normal distributed longitudinal velocities [m/s] taken from the location marked with the red point in the left figure, where the mean velocities are shown. Location: Piv-Box 200, Plane 2, 80 l/s.

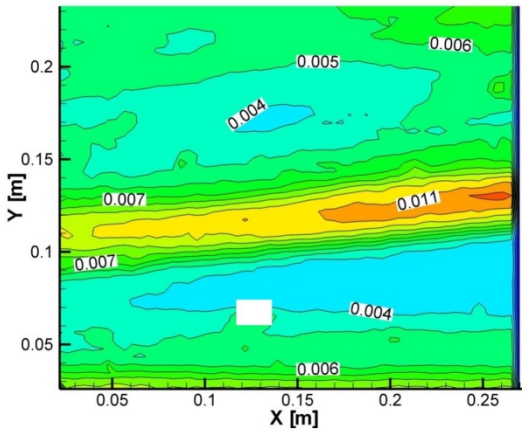

Figure 7 Confidence interval of the mean velocity in longitudinal direction [m/s]

Figure 7 shows the result of the reliability of the mean value of Figure 6. The highest confidence interval is ±0.011 m/s with a longitudinal mean velocity of approximately 2 m/s which indicates a good measurement. For other locations of PIV-measurements (PIV-Box 201 and PIV-Box 202, for all four planes in Figure 2 and Figure 3) equivalent results for the reliability of the mean value (in longitudinal and lateral direction) are achieved. The reliability of the standard deviation is also checked with a χ^2-distribution and shows similar good results as for the mean value (not shown in this paper).

3. VELOCITY CORRECTION FACTOR

Due to the bend upstream of the Y-bifurcator and the short pipe between the bend and the Y-bifurcator (18 times the diameter D) a weak secondary flow is still presented. The simply 1D-consideration of the Bernoulli equation is not valid anymore and a velocity correction factor α is introduced to quantify the axial velocity. Generally, α is defined as (taken from (Preißler & Bollrich, 1980))

$$\alpha = \frac{E_{k,real}}{E_{k,theoretical}} = \frac{1}{u^3\ A} \int^A u_A^3\ dA \qquad (5)$$

whereas $E_{k,real}$ is the kinetic energy of the real flow with velocity u_A, $E_{k,theoretical}$ is the kinetic energy of

the mean velocity u, A is the cross section area and dA the differential cross section area.

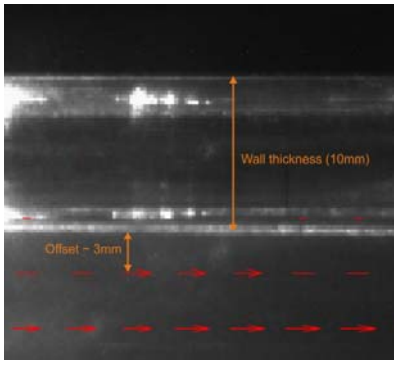

Figure 8 Close up view of the near wall region. The last 3 mm to the wall cannot be measured

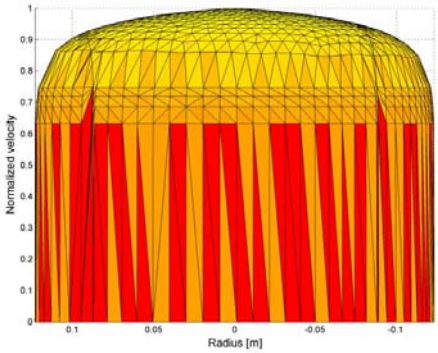

Figure 9 Logarithmic Velocity profile (see Equation 7)

For each PIV-Box four planes (see Figure 3) are used to calculate the velocity correction factor α. To evaluate a single velocity profile Equation 5 needs to be rewritten as

$$\alpha = \frac{1}{u^3 A} \int_{-R}^{+R} u_y^3 \, \pi \, y \, dy \qquad (6)$$

whereas π y is the half circumference, y is the integration variable between the range of –R and +R, u_y is a velocity profile extracted from the four planes in Figure 3 and R is the radius of the pipe. Before Equation 6 will be evaluated one further comment is necessary: In Figure 8 is shown a close-up view of the boundary layer and the first row of evaluated velocity vectors which are 3 mm away from the wall. Due to the reflecting light it is not possible to resolve the last 3 mm and the velocity profile will be closed with a linear function. To estimate the accuracy of this method a 3 dimensional logarithmic velocity profile of a fully turbulent flow with the same Reynolds number is used which is (taken form (Sigloch, 2005), see also Figure 9):

$$\frac{u_{max} - u_{(r)}}{u_\tau} = -\frac{1}{\kappa}\left[ln\left(1 - \sqrt{\frac{r}{R}}\right) + \sqrt{\frac{r}{R}}\right] \qquad (7)$$

whereas u_{max} is the maximum velocity, u_τ is the friction velocity, κ is the von Karman-Constant, R is the pipe radius and u is the velocity at radius r.

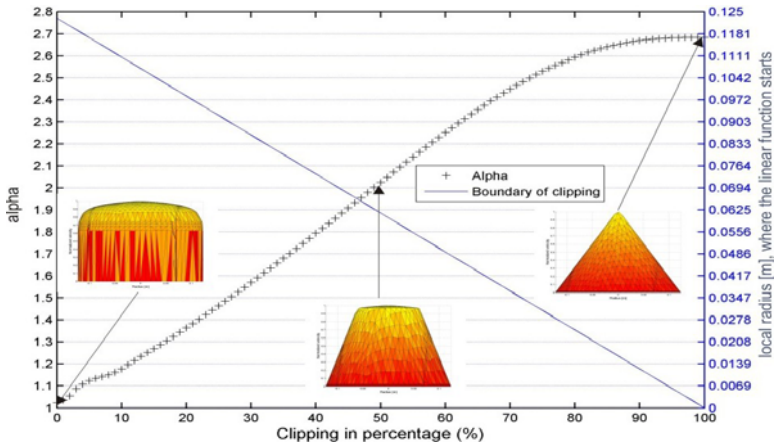

Figure 10 Replacement of the logarithmic velocity profile with a linear function

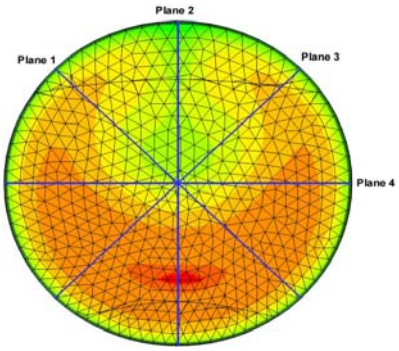

Figure 11 Axial velocities from CFD: 4 lines labelled as Plane 1 to Plane 4 (same position as in Figure 3) are chosen to calculate the α-values

The friction velocity is estimated by using

$$u_\tau \approx 0.2\, Re^{-0.125}\, u_{mean} \qquad (8)$$

whereas Re is the Reynolds number and u_{mean} the mean velocity.

With this generic velocity profile more and more of the logarithmic part will be replaced with a linear function as can be seen in Figure 10. The influence on the calculated α-value with the linear/logarithmic velocity profile is also plotted in Figure 10: At 0% replacement (no linear function) α yields a value of 1.024 (turbulent flow, Re = 10^6), when 100% is substituted with a linear function then the theoretical α value of 2.7 is calculated. For the case where the last 3 mm are replaced with a linear function which correspond to a clipping of 2.4 % (3/R = 3/124=2.4%), a α-value of 1.044 is obtained. Thus, the calculated α-value is only about 2% larger than the "true" value with 1.024. Therefore, it can be expected that the velocity profiles of the secondary flow of the PIV-Measurements plus the linear functions, show similar results as with the logarithmic profile of Equation 7 and the added linear function.

As already mentioned four flow profiles for each PIV-box are used to calculate one single α value of the three dimensional, axial velocity profile. It is therefore necessary to check if the mean value of all four planes is close enough to the exact α value of the whole control section. For that purpose a CFD calculation is done to simulate the secondary flow induced by the bend. The numerical calculation is carried out with Fluent 12.1 with a hybrid mesh of 1.6 million tetrahedron and hexahedron elements. The turbulence model is k-ε with the standard wall function for the near wall treatment. A velocity profile at location "PIV-Box 200" (see Figure 2) will be extracted, to calculate the α value for the whole 3D profile and also for the four lines (see Figure 11). Equation 5 is evaluated to calculate the alpha value for the 3D-Velocity profile and Equation 6 is used to calculate the four α values for the extracted velocities at the blue lines in Figure 11. The results are shown in Table 1: For the 3D-Velocity profile a α-value of 1.043 [-] is obtained and for the mean value 1.042 [-] which is only about 0.1 [%] lower than for the 3D profile. Therefore, it can be expected that the mean of the α-values from the four planes of the PIV-measurement represent the axial secondary flow of the whole 3D profile.

Table 1 Comparison of the velocity correction factor of the entire 3D flow profile and of the mean of the four velocity flow profiles (numerical simulation, location: PIV-Box 200)

3D-Velocity Profile	*Plane 1 - diagonal left*	*Plane 2 - vertical*	*Plane 3 - diagonal right*	*Plane 4 - horizontal*	*Mean of Plane 1 to 4*
-	-	-	-	-	-
1.043	1.026	1.098	1.026	1.018	1.042

The results (discharge 80 l/s) of the PIV-measurement with the linear modification of the near wall region are shown in Figure 12 and Figure 13. Shortly before the flow enters the Y-bifurcator (PIV-Box 201) a weak secondary flow is still visible and the mean value of the four planes for the velocity correction factor α yields 1.037; the velocity factor after the Y-bifurcator (PIV-Box 202) yields a slightly lower value of 1.030. With these α-values the Bernoulli equation (see Equation 1) can be used to calculate the hydraulic loss of the Y-bifurcator including the induced secondary flow of the bend as shown in Figure 14.

4. CONCLUSION

With the use of natural seeding it is possible to carry out PIV-Measurements to investigate the secondary flow up- and downstream of a Y-bifurcator. The quality of this measurement is checked with the velocity lag of the particles which shows that the particles can follow the flow up to a frequency of 1.4 kHz. Additionally, the confidence interval of the mean value of the steady state flow is calculated and confirms the good quality of the results. The secondary flow of the pipe installation is quantified with the velocity correction factor α, based on the velocity profile of several PIV-measurements. Due to the reflection at the inner pipe surface parts of the velocity profile are replaced with a linear function. The calculated α-values, including the linear function, show only a ≈2% deviation in comparison to a complete logarithmic profile without any linear function. The mean value of the calculated α-values for the 2D-Velocity profiles represents accurately enough the 3D-Velocity profile of a control section. This

is double-checked with numerical simulation where the difference between the 2D and 3D-velocity profile is only about ≈0.1%.

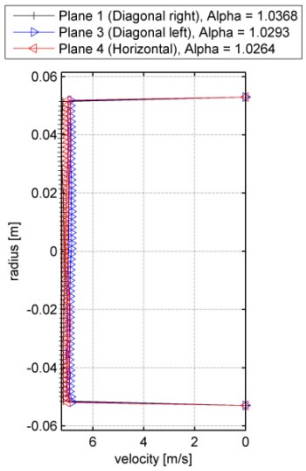

Figure 12 Velocity profile PIV-Box 202

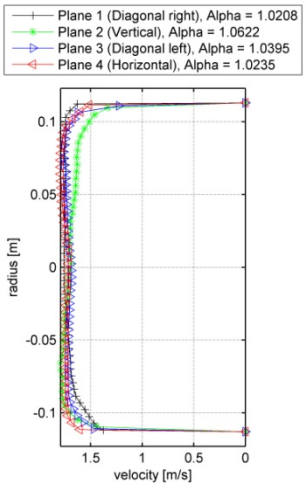

Figure 13 Velocity profile PIV-Box 201

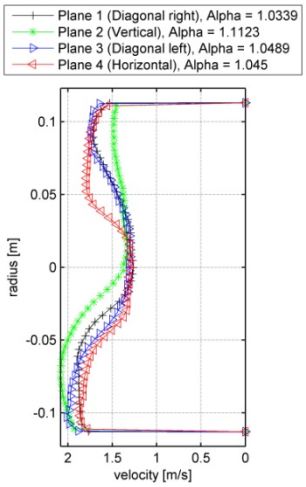

Figure 14 Velocity profile PIV-Box 200

5. ACKNOWLEDGMENTS

This project was funded by Andritz Hydro AG, represented by Mr. Volker Kienberger. The supervisor of the laboratory is Josef Schneider. Many thanks also to J. Woisetschläger for the interesting discussions.

6. REFERENCES

Dobler, W., Knoblauch, H., & Zenz, G. (2010). *Hydraulic investigation of a Bifurcator*. *The First European IAHR Congress* (Vol. The First). Edinburgh.

King, D. L. (1963). *Hydraulic Model Studies of Causey Dam Outlet Works, Weber Basin Project Utah*. *Laboratory Report, Hyd.* (p. 29). Denver.

Lee, B. K., Coleman, H. W., Kim, J. H., & Kwon, H. I. (1993). *Hydraulic model studies of Y-branch*. PROC NATL CONF HYDRAUL ENG, ASCE, NEW YORK, NY(USA)*, 1993,* (p. 1689:1694).

Preißler, G., & Bollrich, G. (1980). *Technische Hydromechanik* (1st ed.). Berlin: VEB Verlag für Bauwesen.

Raffel, M., Willert, C., Wereley, S., & Kompenhans, J. (2007). *Particle Image Velocimetry* (2nd ed.). Springer.

Ruus, E. (1970). *Head losses in wyes and manifolds*. Journal of the Hydraulics Division, 96(3), 593-608.

Sigloch, H. (2005). Technische Fluidmechanik. New York (6th ed., pp. 1-569). Springer-Verlag Berlin Heidelberg.

Williamson, J. V., & Rhone, T. J. (1973). *Dividing flow in branches and wyes*. Journal of the Hydraulics Division, 99(5), 747:769.